### CHAPTER 72

Prediction of the dimensions of a rip current system on a coast with bars

Julio Zyserman<sup>1</sup>, Jørgen Fredsøe<sup>2</sup>, Rolf Deigaard<sup>2</sup>

#### Abstract

A method to determine the dimensions of rip current systems (distance between rip currents, and width and depth of the rip channels) is presented for the case of a coast with longshore bars. The method is based on an overall sediment balance in the nearshore region. The balance is determined by application of a model for the wave-induced flow combined with a sediment transport model. The influence of the wave height, the wave period, and the direction of wave propagation, as well as of the sediment size is analyzed.

#### 1. Introduction

\_\_\_\_\_\_

Rip currents are strong narrow currents flowing seaward across the breaker zone, which return the water transported landward by the breaking waves. These currents influence the characteristics of the wave-induced flow and the associated sediment transport, and thereby the nearshore morphology. While a diversity of analytical and numerical models has been developed to determine the features of rip-current systems on plane beaches, the references regarding rip currents on coasts with longshore bars are rather scarce.

The main purpose of the present paper is to develop a method which can describe the characteristics of a rip-current system on a coast with bars taking an overall balance of the sediment transported in the nearshore region into account.

Laboratorio de Hidráulica Aplicada, INCYTH, Casilla de Correo 21, 1802, Aeropuerto de Ezeiza, Ezeiza, ARGENTINA.

Institute of Hydrodynamics and Hydraulic Engineering, Building 115, Technical University of Denmark, DK-2800 Lyngby, DENMARK.

## 2. The model for the wave-induced flow

#### Hydrodynamics in the uniform condition

Consider the situation shown in Fig. 1. A train of waves propagates obliquely towards a coast with a longshore bar. The bottom contours are straight, and parallel to the shoreline. The adopted system of reference is also shown in the figure. The x-axis is coincident with the still-water shoreline, and the y-axis has its origin at the coast and extends offshore. As the waves approach the coast, the effect of refraction makes the wave fronts turn, and the combined effects of shoaling and refraction do that the waves become steeper, until they break on the bar. The subscript "br" is used to indicate characteristics of a given variable at the line of breaking. The broken waves pass over the crest of the bar to the deeper water of the trough where the process of wave breaking is reduced or completely stopped. As the waves further propagate towards the beach, they are shoaled and refracted until they eventually break on the inner beach.

Under these conditions, a longshore current is generated by the breaking waves. The driving force for the

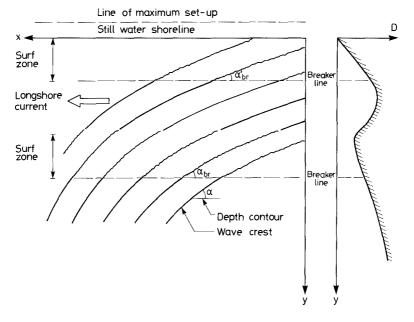


Figure 1. Definition sketch for uniform case.

current is provided by the cross-shore gradient of the shear component of the radiation stress tensor  $S_{\chi\gamma}.$  Since the value of  $\delta S_{\chi\gamma}/\delta \gamma$  is directly proportional to the rate of dissipation of wave energy (Longuet-Higgins, 1972), the forcing term and therefore the induced current will be greater where the dissipation of wave energy is more intense, i.e. in the vicinity of the lines of breaking.

The waves also cause a deviation of the mean water surface from the still water level. Seaward of the breaker line a depression of the mean water level or "set-down" exists, whereas a raise of the water surface with respect to the still water or "set-up" appears in the surf zone.

As an example the velocity profile of the depthintegrated longshore current calculated over a bar-trough profile is shown in Fig. 2.

The calculation have been made for irregular waves, and the wave conditions have been determined by the model of Battjes and Janssen (1978) for the transformation of Rayleigh distributed waves, with the breaker index given by Battjes and Stive (1985).

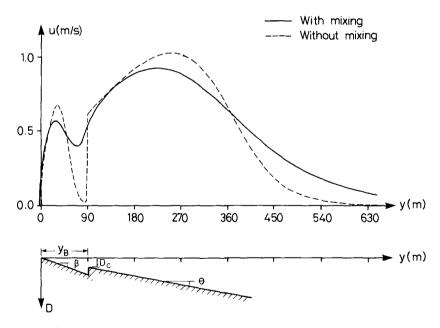


Figure 2. Calculated profiles of longshore current, and the bar-trough profile.

Refraction was determined by application of Snell's law using the peak period of the irregular waves, and disregarding the influence of the currents on wave refraction. Bottom friction was modelled according to Fredsøe (1984), and the turbulent stresses were represented by the usual gradient diffusion of momentum, with the coefficient for lateral exchange of momentum given by Battjes (1983). More details about the representation of the forcing terms can be found in Zyserman (1989).

The variables were chosen as: deep water wave height  $H_{rms,0}=1.2$  m, peak wave period  $T_p=7.5$  s, mean direction of wave propagation in deep waters  $\alpha_0=45^{\circ}$ , distance from still water shoreline to the crest of the bar  $y_B=90$  m, still water depth over the bar  $D_C=1$  m, slope of the inner beach  $\tan(\beta)=0.02$ , slope of the seaward face of the bar  $\tan(\theta)=0.01$ , and mean diameter of the bed material d=0.20 mm. The profile labeled as "without lateral mixing" in Fig. 2 was determined disregarding the cross-shore exchange of momentum.

### Hydrodynamics in the non-uniform condition

Figure 3 shows the non-uniform coastal geometry. The cross section through the bar is similar to the uniform profile considered above, but the bar is interrupted by rip channels of width  $W_H$  and depth  $D_H$ , so that the length of the bar between adjacent holes is  $L_B$ . The rip channels are taken to have a rectangular section, where they cross the bar.

The waves still break on the bar, but the water depth in the channels is so large that the wave breaking here is much less intense than on the bar, if the waves break at all. The tendency to build up the wave set-up is therefore much stronger over the bars than in the channels.

This means that the mean water level is higher behind the bar than at the holes, and that a pressure gradient directed towards the rip channels exists. This pressure gradient will accelerate the mass of water at the trough in the longshore direction, until it turns seaward and flows through the holes in the form of a rip current. The amount of water discharged by the rips is compensated by the water flowing over of the bar into the trough.

The wave-induced currents can be described by means of depth-integrated equations for conservation of x-momentum and of y-momentum and the continuity equation. In the general form these equations read:

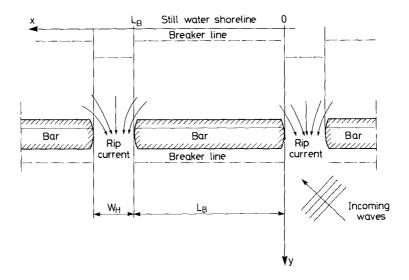


Figure 3. Definition sketch for the non-uniform case.

$$\rho h \left( \frac{\partial U}{\partial t} + U \frac{\partial U}{\partial x} + V \frac{\partial U}{\partial y} + g \frac{\partial \overline{\eta}}{\partial x} \right) + \frac{\partial S}{\partial x} + \frac{\partial S}{\partial y} - \frac{\partial T}{\partial x} - \frac{\partial T}{\partial x} - \frac{\partial T}{\partial y} + \overline{\tau}_{bx}$$

$$= 0 \tag{1}$$

$$\rho h \left( \frac{\partial V}{\partial t} + U \frac{\partial V}{\partial x} + V \frac{\partial V}{\partial y} + g \frac{\partial \overline{\eta}}{\partial y} \right) + \frac{\partial S}{\partial x} + \frac{\partial S}{\partial y} - \frac{\partial T}{\partial x} - \frac{\partial T}{\partial x} - \frac{\partial T}{\partial y} + \overline{\tau}_{by}$$

$$= 0 \tag{2}$$

$$\frac{\partial \overline{\eta}}{\partial t} + \frac{\partial (hU)}{\partial x} + \frac{\partial (hV)}{\partial y} = 0$$
 (3)

where U and V are the time-mean and depth-averaged components of the flow, t is time, h is the total depth h = D+ $\eta$ , D is the local depth measured from the still water level and  $\eta$  is the water surface elevation, g is the acceleration of the gravity,  $S_{xx}$ ,  $S_{xy}$ , and  $S_{yy}$  are the longshore, shear, and cross-shore components of the radiation stress tensor respectively,  $T_{xx}$ ,  $T_{xy}$ , and  $T_{yy}$  are the analogous values of the Reynolds stresses produced by the turbulence, and  $\tau_{bx}$  and  $\tau_{by}$  are the components of the resulting bed shear stress over a wave period.

Solution of equations (1), (2), and (3) gives the three variables U,V, and  $\frac{1}{n}$  in the domain of interest.

A numerical solution of equations (1) to (3) requires large and laborious calculations, and considerable amounts of computing time. It has therefore been preferred to adopt some physically well based simplifying assumptions, in order to reduce the computations involved in the solution. This has been done because a large number of study cases involving different wave characteristics and shore configurations was to be analyzed.

The assumptions adopted are listed below. A detailed discussion of the procedure is given by Zyserman (1989).

- A steady state is considered.
- The diffusion of momentum due to turbulent fluctuations of the velocity is not taken into account.
- It is assumed that the wave characteristics are uniform alongshore between two holes.
- The cross shore discharge of water per unit length over the crest of the bar produced by the breaking waves  $\mathbf{q}_{\mathbf{w}}$  is given by

$$q_{W} = h_{C}V = h_{C} \sqrt{2g(\overline{\eta}_{0} - \overline{\eta})}$$
 (4)

according to Deigaard (1986).  $\bar{\eta}_0$  is the value of the set-up for the uniform situation,  $\bar{\eta}$  is the real value of the set-up, and  $h_c$  is the mean-water depth over the crest of the bar.

It is assumed that the cross-shore component of the current V varies linearly behind the bar, and that cross shore discharge is constant offshore the bar:

$$V = V_{\text{max}} y / y_{\text{B}} \text{ for } 0 \le y \le y_{\text{B}}$$
 (5)

$$hV = constant for y > y_B$$
 (6)

 $\mathbf{V}_{\text{max}}$  being the maximum value of V in the through just behind the bar crest.

- The contribution of the wave set-up  $\overline{\eta}$  to the total depth h is disregarded, so now h = D.
- The mean water surface behind the bar is horizontal.

With these simplifications, the set of three equations can be reduced to the following two partial differential equations:

$$\rho D \left( U \frac{\partial U}{\partial x} + V \frac{\partial U}{\partial y} + g \frac{\partial \overline{\eta}}{\partial x} \right) + \frac{\partial S}{\partial y} + \overline{\tau}_{bx} = 0$$
 (7)

$$\frac{\partial (DU)}{\partial x} + \frac{\partial (DV)}{\partial y} = 0 \tag{8}$$

which can be solved by an iterative procedure.

The numerical solution is performed using a finite difference formulation of Eqs. (7) and (8). The unknowns are determined in a domain having the length of the bar  $L_B$  in the x-direction, and being bounded by the stillwater shoreline and an offshore limit  $y_L$ , which is taken as the position where the value of  $\partial S_{xy}/\partial y$  becomes smaller than a chosen limiting value.

The boundary conditions for the variables are:

$$U = 0 \quad \text{for } y = 0 \quad \text{and} \quad 0 \leqslant x \leqslant L_{B} \tag{9}$$

$$U = 0$$
 for  $y = y_L$  and  $0 \le x \le L_B$  (10)

$$V = 0$$
 for  $y = 0$  (11)

DV = constant for 
$$Y_R \le y \le y_L$$
 (12)

The boundary condition for  $\frac{1}{\eta}$  is determined from the expansion-loss of the rip current flowing through the rip channels:

$$\bar{\eta}_{\rm H} = \frac{|\vec{\nabla}_{\rm rip}|^2}{2q} \tag{13}$$

The subscript "H" indicates a value of the variable determined at the hole,  $\bar{v}_{\text{rip}}$  is the velocity in the rip channel.

Figure 4 shows the longshore current velocity profiles obtained for  $\rm H_{rms,\,0}$  = 1.2 m,  $\rm T_p$  = 7.5 s,  $\alpha_0$  = 45°,  $\rm tan(\beta)$  = 0.02,  $\rm tan(\theta)$  = 0.01,  $\rm D_c$  = 1 m,  $\rm L_B$  = 180 m,  $\rm Y_B$  = 90 m,  $\rm W_H$  = 22.5 m,  $\rm D_H$  = 3 m, and d = 0.2 mm. The velocity in the rip channel equals 1.22 m/s in this situation.

The results obtained can be compared with the velocity profile without lateral mixing of Fig. 2. The same data were used in the two examples, so the observed differences are due to the presence of the rip currents.

A striking difference is the smoothness of the velocity profiles in the case of non-uniform flow conditions, even when the effect of turbulent momentum transfer is disregarded. This is due to the cross shore flow which effectively transfers longshore momentum in the

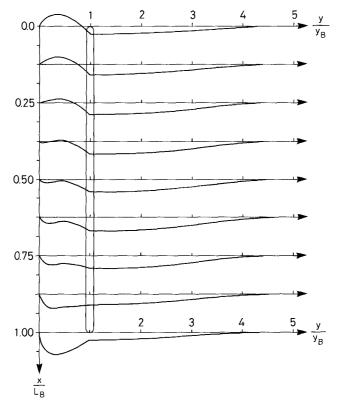


Figure 4. Calculated longshore current flow in presence of rip currents.

cross shore direction. The shore parallel velocities on the bar are reduced because water from offshore continously is moving into the field of driving forces from the wave breaking. Similarly the longshore momentum is convected into the trough, giving a continuous velocity profile.

The flow model which gives the flow field and the wave conditons in the near-shore area is used as basis for the sediment transport calculations.

### 3. The sediment transport model

The model used to calculate sediment transport has been described in detail in a series of papers by Freds $\phi$ e, Andersen, and Silberg (1985), and Deigaard, Freds $\phi$ e, and Hedegaard (1986a, 1986b), so only the main features of the model are presented here.

The total load transport of sediment per unit width  $q_{\rm t}$  is determined as the sum of two contributions: the bed load transport  $q_{\rm b}$  and the suspended load transport  $q_{\rm s}$ .

The instantaneous bed load transport is related to the instantaneous dimensionless bed shear stress or Shield's parameter  $\theta$  according to the findings of Engelund and Fredsøe (1976).  $\theta$  is determined at each instant from the model developed by Fredsøe (1984) for the boundary layer in combined wave-current situations. The mean value of the bed transport during a wave period is then found by integration of the instantaneous values.

The concentration profile of suspended sediment is determined at every instant by solving the diffusion equation for the sediment. The turbulent exchange factor for the suspended sediment is taken equal to the eddy viscosity of the flow. The turbulent eddy viscosity is determined as the combination of contributions from the current boundary layer, the wave boundary layer and from the wave breaking.

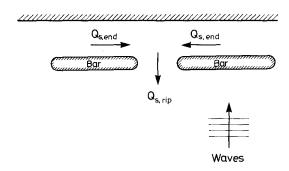
The mean value of the suspended transport in the direction of the mean current over a wave period is determined by time-averaging the product between the concentration of suspended sediment and the total (current + wave) horizontal velocity in the direction of the current. This product is integrated between the bed level and the water surface to give the transport rate.

# 4. The prediction of the dimensions of the rip-current system

Based on the sediment transport calculations the dimensions of the bar-rip channel system is determined. The dimensions considered are: the bar length  $L_{\rm B}$ , the width of the rip channel  $W_{\rm H}$  and the depth  $D_{\rm H}$  of the rip channel. The geometry of the system is then determined for a given bar profile, sediment characteristics and incoming wave conditions. Equilibrium conditions are assumed and no erosion or deposition must occur. The basis for the analysis are the sediment budgets for two cells, Fig. 5.

The sediment transported in the trough by the longshore currents flowing toward the rip must equal the amount of sediment flushed through the hole by the rip. This condition can be written as:

$$Q_{S,rip} = Q_{S,end}$$
 (14)



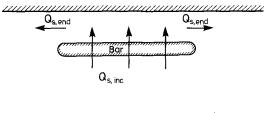




Figure 5. Sediment balances.

The total amount of sediment transported over the bar must be equal to the amount of sediment transported toward the rip, giving:

$$Q_{S,inc} = Q_{S,end}$$
 (15)

where the the sediment transport per unit width  $q_t$  has been integrated along the bar, and across the rip channel and the trough, in order to determine  $Q_{S,inc}$ ,  $Q_{S,rip}$ , and  $Q_{S,end}$ , respectively.

These two conditions make it possible to determine the bar length  $L_B$  and rip depth  $D_H$  for a given value of the rip width  $W_H$ . The solution is made by iteration, calculation the ratio between the in- and outgoing sediment of each cell. An example of the calculations is shown in Fig. 6 with the following input data:  $H_{\text{rms},0}=1.2~\text{m}$ ,  $T_p=7.5~\text{s}$ ,  $\overline{\alpha}_0=0^{\circ}$ ,  $\tan(\beta)=0.02$ ,  $\tan(\theta)=0.01$ ,  $D_C=1~\text{m}$ ,  $L_B=$  variable,  $Y_B=90~\text{m}$ ,  $W_H=22.5~\text{m}$ ,  $D_H=$  variable, and

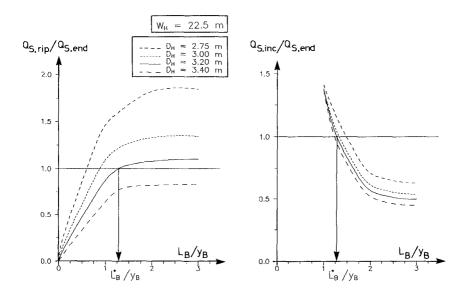


Figure 6. The determination of the length of the bar.

d = 0.2 mm. The solution in this case is found for  $\rm D_{H}$  = 3.2 m and  $\rm L_{R}$  = 1.3  $\rm y_{R}$  = 120 m.

When this method is applied for different widths of the hole  $W_H$ , it is possible to obtain a set of curves representing the equilibrium length of the bar  $L_B$ , the depth of the hole  $D_H$ , and the total sediment transport of the rip  $Q_{\rm S,rip}$  as functions of the width of the hole  $W_H$ , for a given wave situation, bar-trough profile, and bed material. Fig. 7 shows the equilibrium value of  $Q_{\rm S,rip}$  and  $D_H$  as function of and the width of the hole. The data are similar to Fig. 6, except for the wave approach angle which is now  $\alpha_0=45^{\rm O}$ . The equilibrium bar length is very insensitive to changes in  $W_H$  being constant about  $L_B=1.37$   $y_B=123$  m.

 $Q_{\rm S,rip}$  is a measure of the flushing capacity of rip channel, and the situation with maximum  $Q_{\rm S,rip}$  can therefore be taken as the optimal configuration where the rip current has the highest capacity to flush sediment in the seaward direction. This criterion gives a rip channel width of  $W_{\rm H}$  = 25 m and a depth of  $D_{\rm H}$  = 2.8 m.

A sensitivity analysis has been made to illustrate the influence that the wave height, the wave period, and the diameter of the bed material have on the solution. The situation illustrated in Fig. 7 with  $\bar{\alpha}_0$  =

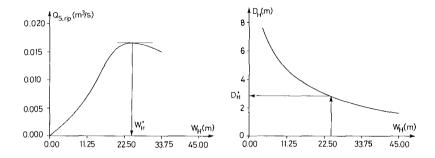


Figure 7. The determination of the dimensions of the rip channels based on  $(Q_{S,rip})^{max}$ .

 $45^{\rm O}$  is taken as Case I, and used as a basis for the comparison. All the other cases are obtained by changing the value of one of the independent variables with respect to its value in this case. Case II is the situation already considered in which the angle of wave incidence was changed to  $\alpha_0=0^{\rm O}$ . In Case III the wave height is taken as  $H_{\rm rms},_0=2$  m. In Case IV the wave period is taken as  $T_p=10$  s, and in Case V the grain size is taken as d=0.4 mm, giving w = 0.05 m/s. The results are presented in Table 1.

An alternative criterion for determining the rip channel width has been proposed by Skou and Fredsøe (1990). The idea is that nature should select the

Case	Hrms,0	T <sub>p</sub> (s)	$(^{\circ})$	d (mm)	$L_{ m B}$ (m)	W <sub>H</sub> (m)	D <sub>H</sub> (m)
I	1.2	7.5	45	0.20	123	25	2.80
ΙI	1.2	7.5	0	0.20	120	25	3.00
III	2.0	7.5	45	0.20	146	11	5.25
IV	1.2	10.0	45	0.20	126	23	3.15
V	1.2	7.5	45	0.20	123	43	1.65

 $D_C = 1 \text{ m}$   $Y_B = 90 \text{ m}$   $tan(\beta) = 0.02$   $tan(\theta) = 0.01$ 

Table 1. The equilibrium dimensions as function of the input parameters.

condition giving the maximum slope of the  $\Omega_{S,rip}$  -  $W_H$  curve, as this represents the maximum strength of the response of the system to a perturbation imposed on it. If for instance the width of the channel is reduced by a random infill of sediment, then the increase of  $\Omega_{S,rip}$  due to the decrease in  $W_H$  is a measure of how fast the rip channel will erode to reestablish the equilibrium. Fig. 8 illustrates the application of this criterion to Case III, giving  $W_H$  = 17.6 m and  $D_H$  = 3.6 m.

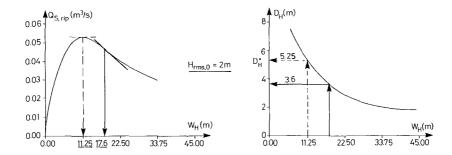


Figure 8. Determination of the dimensions of the rip channels based on  $(dQ_{S,rip}/dW_H)_{max}$ .

## 5. Conclusions

A method for determining the features of a stable shore when a rip-current system exists on a bar-trough shore profile has been developed. The calculated characteristics of the coast comprise the length of the bar or spacing between rip currents  $\mathbf{L}_{\mathbf{B}}$ , and the dimensions of the rip channel: width  $\mathbf{W}_{\mathbf{H}}$  and depth  $\mathbf{D}_{\mathbf{H}}$ .

The method reproduces some characteristics of the rip-current systems that can be observed in nature fairly well, such as the larger distance between rip channels and the deeper holes associated with heavy breakers, see Case III of Table 1.

No perceptible influence of the grain diameter on the length of the bar was found, but coarser grains led to wider and shallower holes. It was also determined that waves of normal incidence produce slightly shorter bars and deeper holes than waves of oblique incidence.

#### 6. References

- Battjes, J.A. and Janssen, J.P.F.M. (1978): Energy loss and set-up due to breaking of random waves. Procs. 16th. Int. Conf. on Coast. Eng., Hamburg, Vol. 1, pp. 569-587.
- Battjes, J.A. and Stive, M.J.F. (1985): Calibration and verification of a dissipation model for random breaking waves. Jour. fo Geophys. Res., Vol. 90, No. C5, pp. 9159-9167.
- Battjes, J.A. (1983): Surf zone turbulence. Procs. of Seminar on Hydrodynamics of Waves in Coastal areas. I.A.H.R., Moscow, U.S.S.R., pp. 137-140.
- Deigaard, R. (1986): Longshore current behind bars. Prog.
- Rep. 64, ISVA, Techn. Univ. of Denmark, pp. 25-29. Deigaard, R., Fredsøe, J. and Hedegaard, I.B. (1986a): Suspended sediment in the surf zone. Jour. of Waterway, Port, Coast. and Ocean Eng., ASCE, Vol. 112, No. 1, pp. 115-128.
- Deigaard, R., Fredsøe, J. and Hedegaard, I.B. (1986b): Mathematical model for littoral drift. Jour. of Waterway, Port, Coast. and Ocean Eng., ASCE, Vol. 112, No. 3, pp. 351-369.
- Engelund, F. and Fredsøe, J. (1976): A sediment transport model for straight alluvial channels. Nordic Hydrology, Vol. 7, pp. 293-306.
- Fredsøe, J. (1984): Turbulent boundary layer in wavecurrent motion. Jour. of Hydr. Eng., ASCE, Vol. 110, pp. 1103-1120.
- Fredsøe, J., Andersen, O.H., and Silberg, S. (1985): Distribution of suspended sediment in large waves. Jour. of Waterway. Port, Coast. and Ocean Eng., ASCE, Vol. 111, No. 6, pp. 1041-1059.
- Longuet-Higgins, M.S. 81972): Recent progress in the study of longshore currents. In: Waves and Beaches and Resulting Sediment Transport. Edited by R.E. Meyer. Academic Press, pp. 203-248.
- Skou, A. and Fredsøe, J. (19 $\overline{90}$ ): Application of the Escoffier curve to determine cross section areas of tidal inlets. Prog. Rep. 71, ISVA, Techn. Univ. of Denmark, pp. 51-60.
- Zyserman, J.A. (1989): Characteristics of stable rip current systems on a coast with a longshore bar. Series Paper 46, ISVA, Techn. Univ. of Denmark, 178 pp.
- Zyserman, J.A., and Fredsøe, J. (1988). The influence of rip currents on the longshore sediment transport. Procs. of the 2nd Int. Symposium on Wave Res. and Coastal Eng. Published by the Special Research Group 205 of the University of Hannover, pp. 125-138.